Research in Astron. Astrophys. **2013** Vol. **13** No. **5**, 547–556
http://www.raa-journal.org *http://www.iop.org/journals/raa*

Research in Astronomy and Astrophysics

DEFPOS Hα observations of the W80 Complex

Nazim Aksaker

Vocational School of Technical Sciences, University of Çukurova, Adana, Turkey
Research and Application of Space Sciences and Solar Energy Center (UZAYMER), University of Çukurova, Adana, Turkey; *naksaker@cu.edu.tr*

Received 2012 November 14; accepted 2012 December 13

Abstract We present Hα emission line measurements of the W80 nebula complex. A total of 26 regions have been observed inside the nebula with the Dual Etalon Fabry-Perot Optical Spectrometer system at the f/48 Coudé focus of the 150 cm RTT150 telescope located at TUBITAK National Observatory in Antalya, Turkey. The intensities, local standard of rest velocities, heliocentric radial velocities and linewidths for full width at half maximum of the Hα emission lines have been determined from these observations. They lie in the range of 259 to 1159 Rayleigh (R; 1R = $10^6/4\pi$ photons cm^{-2} sr^{-1} s^{-1} = 2.41×10^{-7} erg cm^{-2} sr^{-1} s^{-1} at Hα), 4 to 12 km s^{-1}, –3 to –11 km s^{-1} and 44 to 55 km s^{-1}, respectively. The radial velocity measurements show that there are several maxima and minima inside W80. The new results confirm findings in the literature that the complex seems to be rather uniform in terms of radial velocity and no turbulent motion is seen inside the complex. The average value of the calculated emission measure for the region is 3.1 pc cm^{-6}.

Key words: instrumentation: interferometers — ISM: H II regions — techniques: radial velocities — techniques: interferometric

1 INTRODUCTION

The North America (NGC 7000) and Pelican (IC 5070) Nebulae complex, together cataloged as W80 (Westerhout 1958), is $\sim 3^\circ$ east-southeast of Deneb in Cygnus. The region is located along the line of sight of the Cyg OB6 and OB7 associations which are part of a structure known as the Cygnus superbubble (Uyanıker et al. 2001). According to a recent study, an O5V star (2MASS J205551.25+435224.6) is located close to the geometric center of the complex (Comerón & Pasquali 2005). In the same paper, an assumed distance of 610 pc is given for the exciting source of W80. Straižys & Laugalys (2008) have identified a few more possibly highly reddened O-type stars that contribute to the ionization of the North America and Pelican nebulae. These two regions (NGC 7000 and IC 5070) are separated by a dust lane, L935 (Lynds 1962), which lies in the north-south direction.

The W80 nebula complex, as a classical H II region, is very important for understanding the nature (physical structure, kinematics etc.) of such structures. Studying H II regions helps us to determine their sources of ionization (Aksaker et al. 2011) and to understand how these regions are related to the general structure of the ISM (Reynolds et al. 1998; Hausen et al. 2002). Therefore, observing H II regions in a visual band using an Hα emission line gives valuable information (Aksaker et al. 2011; Fich et al. 1989). However, it is difficult to make accurate measurements of line fluxes by using traditional long-slit spectroscopic techniques, because of the low surface brightness and spatially extended emissions from large H II regions. Instead, high resolution spectral analysis of these faint, spatially extended sources requires high sensitivity and wide fields of view (FOVs) for spectrometers, examples of which are the Dual Etalon Fabry Perot Optical Spectrometer (DEFPOS) (Sahan et al. 2005; Şahan et al. 2009; Aksaker et al. 2009) and the Wisconsin H-Alpha Mapper (WHAM) (Tufte 1997; Haffner et al. 2003).

The radial velocity with respect to the local standard of rest ($V_{\rm LSR}$), the full width at half maximum (FWHM), and the intensity of the Hα emission line are obtained very precisely by DEFPOS observations. $V_{\rm LSR}$ can be used for investigating the internal mechanisms such as the turbulence and inhomogeneities (Courtès et al. 1962; Williamson 1970). Measuring the FWHM of the Hα and another emission line from a heavier atom (e.g. N^+ or S^+) can be used to separate thermal from nonthermal motions in the gas (Reynolds 1988). The measured intensity of Hα provides a value of the emission measure (EM) along the line of sight, which can be used in conjunction with the scattering measure, rotation measure and dispersion measure to study interstellar turbulence (Tufte et al. 1999; Haffner et al. 1998). These data help us to understand properties such as the nature of H II regions and the warm ionized medium.

The layout of this paper will be as follows: In the first part, observations (Sect. 2.1) and data reduction (Sect. 2.2) are given. Then, $V_{\rm LSR}$ for these regions is estimated in Section 3.1. The FWHM and its intensity are estimated in Sections 3.2 and 3.3, respectively. Our conclusions and some suggestions for future work are given in the last section.

2 OBSERVATIONS AND DATA ANALYSIS

2.1 Observations

The observations were obtained using the DEFPOS instrument on 2010 September 18–20 at the TUBITAK National Observatory (TUG), Antalya, Turkey. The DEFPOS spectrometer measures the Hα emission line covering a 200 km s^{-1} (4.4 Å) spectral window with a spectral resolution of $\sim$ 30 km s^{-1} and an FOV of $4'$. Detailed information about the instrument, optics, the methods of data analysis, and the related intensity calibration can be found in our earlier works (Sahan et al. 2005; Şahan et al. 2009; Aksaker 2009; Aksaker et al. 2009).

A total of 26 regions were selected in the W80 complex by examining the bright regions from the Digitized Sky Survey[1] (DSS). Thus, a high signal-to-noise ratio (SNR) was obtained in the observations. Present observations covered the bright part of the W80 complex with seven regions belonging to IC 5070 and the rest to NGC 7000. Exposure times were selected to be 2400 s in order to reach an optimum SNR. A journal of observations, including the region ID numbers (Col. (1)), coordinates (Cols. (2) & (3)) and observation dates (Col. (4)), is given in Table 1. The observations are also shown as turquoise circles on the DSS image of the region in Figure 1.

2.2 Data Reduction

The observations were recorded by the 2048$\times$2048 CCD camera mounted on RTT150 and DEFPOS as described in Şahan et al. (2009). The instrumental effects must be removed from the resulting CCD images before any data analysis can occur. This process requires a series of steps including dark, bias, and flat field corrections, to remove the effects of cosmic rays, bad columns, and spurious reflections due to the optical system in DEFPOS. Reduced circular CCD images are then converted to one dimensional Hα spectra with 50 data points in each row by implementing a ring summing procedure (Coakley et al. 1996). A data reduction pipeline for DEFPOS spectra is available in Interactive Data Language (IDL) as described in Aksaker (2009) and Şahan et al. (2009). A sample reduced CCD image and its final spectrum are shown in Figure 2.

[1] *http://skyview.gsfc.nasa.gov/*

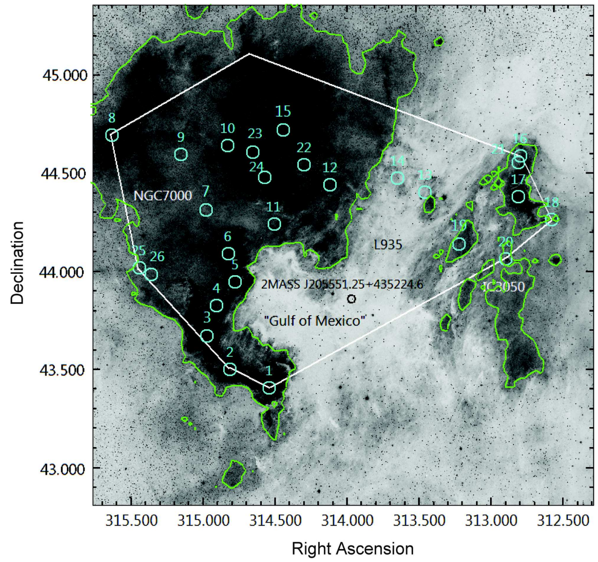

Fig. 1 Optical image of the W80 region (DSS image) that is comprised of two HII regions, NGC 7000 (North America Nebula) and IC 5070 (Pelican Nebula), with the dark lane L935 separating them. Turquoise circles show the relative size and positions of the observed regions. The black circle near the center marks the position of the exciting source identified by Comerón & Pasquali (2005). The irregular polygon in the region being investigated shows the area modeled by DEFPOS data, corresponding to the field shown in Fig. 4. The green contour lines were obtained from the brightness value of the DSS image to show borders of the nebulae. The coordinates are J2000 decimal degrees.

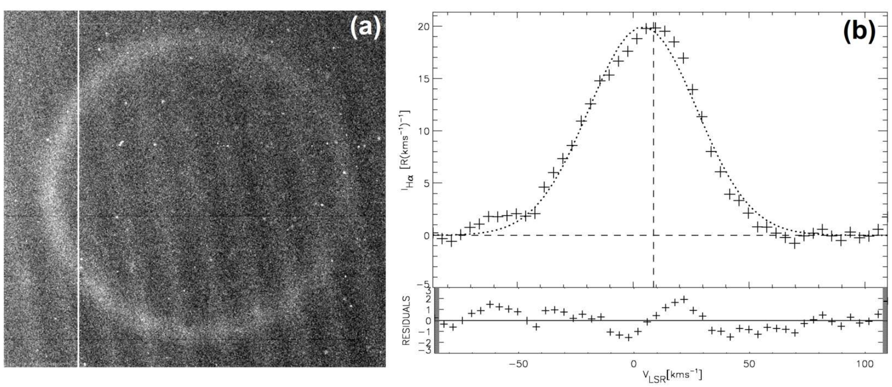

Fig. 2 The brightest regions inside W80 were selected as a target and are described in Table 2. (a) A sample CCD image taken on 2010 September 19. (b) The top panel shows the spectrum and bottom panel shows the residuals of the fit. The spectrum consists of 50 spectral elements, each corresponding to a 200 km s^{-1} spectral window. The real spectrum and the best fit spectrum to the real spectra are shown with + symbol and dotted line respectively (a + symbol represents 4 km s^{-1}, which is equivalent to 0.087 Å in wavelength). The dashed horizontal bar defines the zero level (see the text for further details).

Table 1 Journal of Observations (exposure time = 2400 s)

Region Number	Coordinates α_{2000} (h: m: s)	δ_{2000} (°: ′: ″)	Observation Date
1	20:58:10	43:24:59	2010 Sep. 18
2	20:59:17	43:30:32	2010 Sep. 18
3	20:59:56	43:40:34	2010 Sep. 18
4	20:59:41	43:50:02	2010 Sep. 18
5	20:59:10	43:57:19	2010 Sep. 18
6	20:59:22	44:05:52	2010 Sep. 18
7	21:00:00	44:19:05	2010 Sep. 18
8	21:02:44	44:41:35	2010 Sep. 18
9	21:00:44	44:36:01	2010 Sep. 18
10	20:59:24	44:38:56	2010 Sep. 18
11	20:58:04	44:15:10	2010 Sep. 18
12	20:56:29	44:27:08	2010 Sep. 19
13	20:53:46	44:24:51	2010 Sep. 19
14	20:54:33	44:29:10	2010 Sep. 19
15	20:57:49	44:43:51	2010 Sep. 19
16	20:51:02	44:35:33	2010 Sep. 19
17	20:51:06	44:23:10	2010 Sep. 19
18	20:50:10	44:15:49	2010 Sep. 20
19	20:52:49	44:08:44	2010 Sep. 20
20	20:51:29	44:04:07	2010 Sep. 20
21	20:51:05	44:33:29	2010 Sep. 20
22	20:57:13	44:33:10	2010 Sep. 20
23	20:58:41	44:37:03	2010 Sep. 20
24	20:58:20	44:29:24	2010 Sep. 20
25	21:01:53	44:01:08	2010 Sep. 20
26	21:01:32	43:59:20	2010 Sep. 20

The SNR of a spectrum, which is derived from an image, can be calculated as the ratio of the amplitude of the Hα line to the amount of scatter in the residuals. The 2400 second integration time provides an SNR of $\simeq$ 20 for a 900 R line. Details of the calculation of the SNR for data taken by DEFPOS can be found in Aksaker (2009).

By using a fitting program, the best Gaussian profile for each spectrum was obtained and the best curve fitting for the data is shown in Figure 2. The value of the coefficient of determination is R^2=0.984, where R^2=1 corresponds to a profile with a perfect regression fit. The intensity, radial velocity and line width of each Hα spectrum were defined with the same procedure.

The real data points and their best fitting spectral shape are shown with (+) symbols and the dotted line in Figure 2(b), respectively. In all Hα spectra, the horizontal axis is expressed in terms of the velocity scale (km s^{-1}) and the vertical axis is the intensity in terms of [R (km s^{-1})$^{-1}$]. The radial velocities are given with respect to the Local Standard of Rest (LSR) which is shown with a vertical dashed line at 8.9 km s^{-1} in Figure 2(b). The velocity calculated from these Hα data with respect to the LSR ($V_{\rm LSR}$) is about 4.2$\pm$0.5 km s^{-1}. Its line width arising from the FWHM is convolved to result in a velocity value $V_{\rm LSR}$ of 54.7$\pm$1.4 km s^{-1}. The corresponding intensity of the Hα line is 1159.4$\pm$45.6 R.

The center of the geocoronal Hα is known to be shifted by –2.33 km s^{-1} from the rest wavelength of the recombination line at 6562.82 Å (Haffner et al. 2003; Aksaker et al. 2009). Thus, the LSR velocity values were corrected by $V_{\rm LSR} = -V'_{\rm LSR} - 2.33$ km s^{-1}. $V'_{\rm LSR}$ was computed from the velocity value of the best fit.

The instrumental line width of DEFPOS itself was measured earlier to be 29.5 km s^{-1} using a Thorium-Argon (Th-Ar) hollow cathode lamp. This value is very close to 30 km s^{-1}, the instrumental resolution of DEFPOS over the spectral window near the Hα. Therefore, the line width values are

Table 2 DEFPOS Hα Observations from the W80 Nebula Complex

Region	Intensity (R)	FWHM (km s^{-1})	$V_{\rm LSR}$ (km s^{-1})	$V_{\rm HEL}$ (km s^{-1})	log(EM) (pc cm^{-6})
1	1035.7±50.6	52.9±1.7	8±0.6	−8.0±0.6	3.4
2	953.1±43.3	53.1±1.5	10.7±0.5	−5.2±0.5	3.3
3	1031.7±37.7	50.7±1.3	12.5±0.4	−3.4±0.4	3.4
4	692.6±29.6	52.6±1.4	11.3±0.5	−4.6±0.5	3.2
5	846.3±31.9	46.9±1.2	12±0.4	−3.9±0.4	3.3
6	974.7±38.1	47.6±1.3	10.9±0.4	−5.0±0.4	3.3
7	436.8±27.4	45.3±2.0	10.6±0.7	−5.3±0.7	3.0
8	594.5±30.6	48.9±1.7	4.9±0.6	−10.9±0.6	3.1
9	424.8±34.7	46.5±2.5	6.7±0.9	−9.2±0.9	3.0
10	721.1±39.6	51.7±1.8	4.4±0.6	−11.5±0.6	3.2
11	586.7±35.4	49.0±1.9	9.3±0.7	−6.7±0.7	3.1
12	813±34	51.7±1.4	8±0.5	−8.0±0.5	3.3
13	342.9±32	47.4±3.6	5.9±1.1	−10.2±1.1	2.9
14	259.8±26.5	45.7±3.1	5.5±1.1	−10.6±1.1	2.8
15	1159.4±45.6	54.7±1.4	4.2±0.5	−11.8±0.5	3.4
16	537.7±34.5	50.7±2.1	7±0.7	−9.2±0.7	3.1
17	850.7±40.1	55.5±1.6	5.6±0.6	−10.6±0.6	3.3
18	324.1±34.1	52.2±3.7	11.8±1.3	−4.5±1.3	2.9
19	447.8±49.9	48.8±4.0	8.9±1.3	−7.3±1.3	3.0
20	360.6±25.3	48.2±2.2	8.3±0.8	−7.9±0.8	2.9
21	472±25.1	48.9±1.7	6.2±0.6	−10.0±0.6	3.0
22	678.3±32.5	49.9±1.5	8.7±0.6	−7.3±0.6	3.2
23	764.3±39.2	48.6±1.6	5.9±0.6	−10.0±0.6	3.2
24	1019.9±47.4	61.5±1.8	11.2±0.6	−4.8±0.6	3.4
25	290.2±29.8	46.8±3.1	5.2±1.1	−10.6±1.1	2.8
26	351.2±29.3	44.3±2.4	8.5±0.9	−7.3±0.9	2.9

convolved by using a line fitting program and the intrinsic line widths are estimated by the quadratic subtraction of the 30 km s^{-1} instrumental line width (Aksaker et al. 2009).

In order to perform the intensity calibration for the DEFPOS data, a standard nebular source was used each night before the observations. All calibrations were then tied to an absolute intensity measurement of the central part of NGC 7000 at $\alpha = 20^{\rm h}58^{\rm m}04^{\rm s}.0$, $\delta = +44^\circ35'43''.0$ (equinox=2000.0) within a $\sim 4'$ spatial resolution. The Hα surface brightness at this point is about 900 R within the beam as measured by Aksaker et al. (2009).

3 RESULTS

The intensity ($I_{\rm H\alpha}$ in R), radial velocity (expressed as $V_{\rm LSR}$ and $V_{\rm HEL}$), and line width (expressed as FWHM) of Hα emission lines measured from the W80 complex are given in Table 2, together with their ID numbers (Col. (1)) and EM values, which are given in a logarithmic scale (last column). $V_{\rm HEL}$ values were calculated using the equatorial coordinates and $V_{\rm LSR}$. Errors due to the scatter in the spectral data points have been determined by calculating the standard deviation using a least-squares Gaussian fitting program. All 26 DEFPOS spectra from the W80 complex with their associated fits are shown in Figure 3. All spectra are plotted on the same scale to clearly show the differences. The properties of the regions are further described below.

To complete the analysis, we also constructed two dimensional maps of intensity, $V_{\rm LSR}$ and FWHM using the data with interpolation techniques. Corresponding maps are given in Figure 4. The maps were obtained with the help of TRIANGULATE and TRIGRID functions written in IDL using the observations.

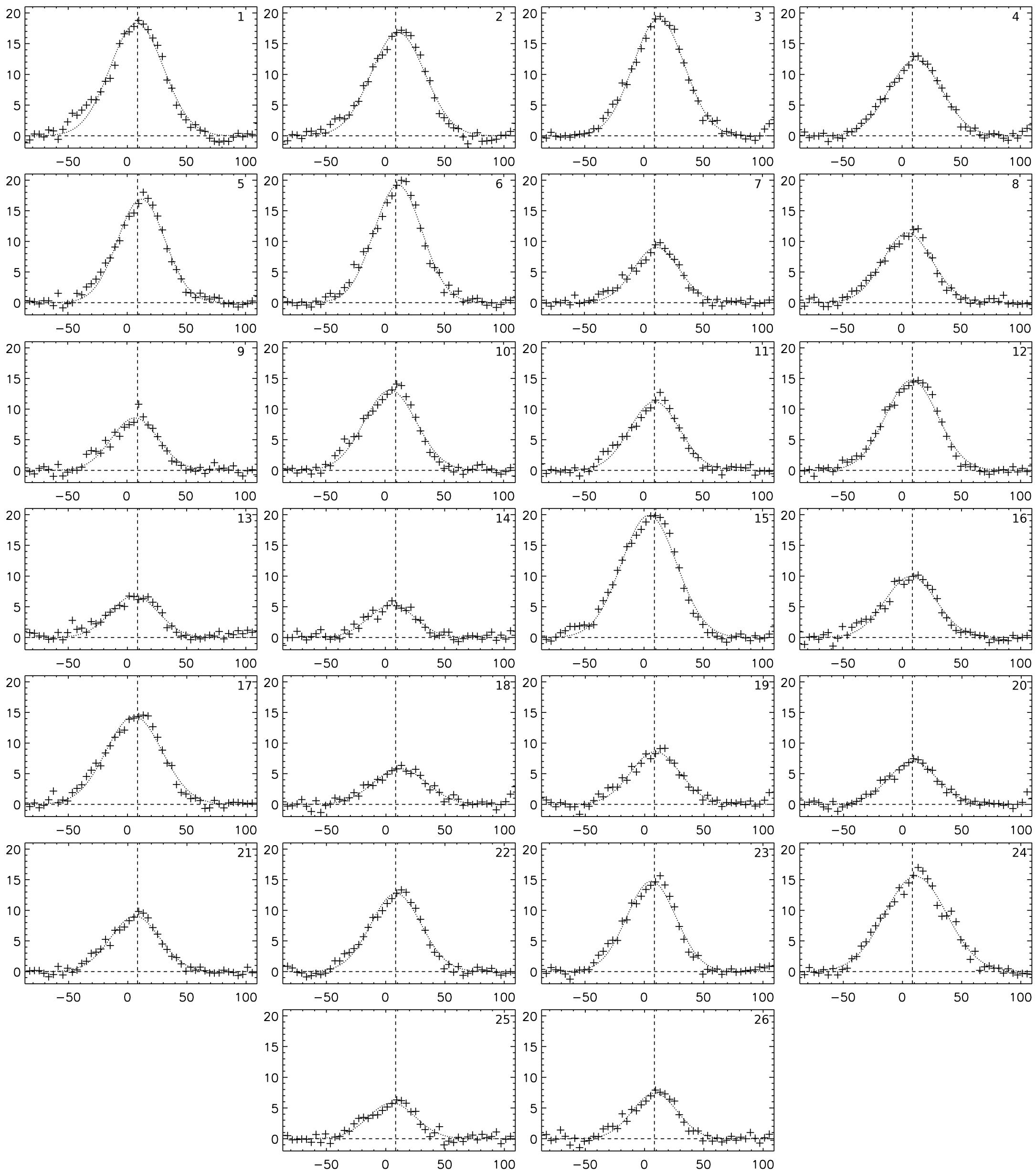

Fig. 3 DEFPOS spectra (velocity [km s^{-1}] versus intensity [R (km s^{-1})$^{-1}$]) of the W80 nebula complex, with their region numbers as given in Tables 1 and 2, shown in their upper right corners.

3.1 The V_{LSR}

All the radial velocities are presented with respect to the LSR. The systematic uncertainties in the data are typically 2–3 km s^{-1}. The contribution to this uncertainty from the velocity calibration that is random noise represents less than 2 km s^{-1} (see Table 2), the same as in previous works

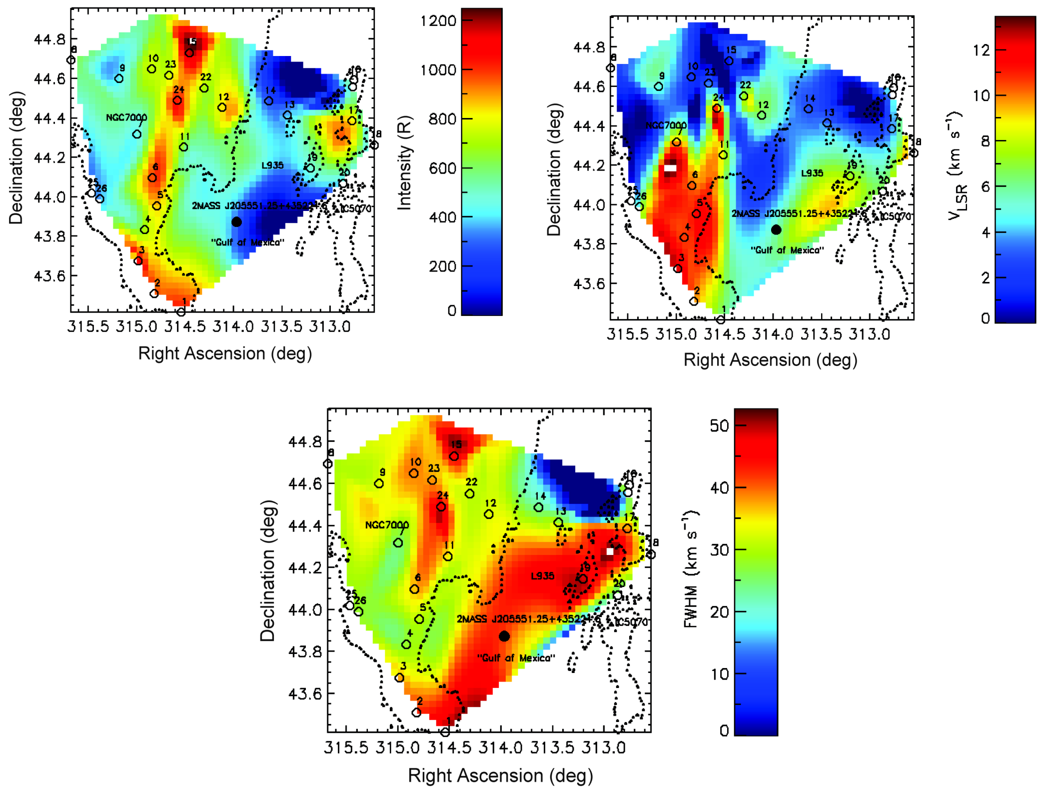

Fig. 4 Interpolation maps of the W80 complex using the measured intensity, $V_{\rm LSR}$ and FWHM data. The areas identifying IC 5070, L935, NGC 7000, observed regions and dotted contour lines are in the same locations as Figure 1.

(Aksaker et al. 2009; Aksaker 2009). The average radial velocity ($V_{\rm LSR}$) is 8.5±0.6 km s^{-1} for NGC 7000, 7.4±0.9 km s^{-1} for IC 5070 and 8.2±0.7 km s^{-1} for the entire W80 complex. Also, the average radial velocity ($V_{\rm HEL}$) is –7.4±0.6 km s^{-1} for NGC 7000, –8.8±0.9 km s^{-1} for IC 5070 and –7.8±0.7 km s^{-1} for the entire W80 complex.

One can accept that these values could be taken as the velocity of NGC 7000 with respect to the LSR. In general, inside both the NGC 7000 and IC 5070 complexes, the radial velocities decrease towards the north. There are several maxima and minima inside NGC 7000. The radial velocity of the periphery of the "Gulf of Mexico" region is almost the same as the average radial velocity. The fastest radial velocity is 12.5±0.4 km s^{-1} (region 3) towards the south of NGC 7000, near the Gulf of Mexico, and the slowest is 4.2±0.5 km s^{-1} towards the north of NGC 7000. Average values for NGC 7000 of 8.5±0.6 km s^{-1} and for IC 5070 of 7.4±0.9 km s^{-1} are quite near each other and differences between NGC 7000 and IC 5070 are less than the uncertainties involved. We can conclude that W80 seems to have a rather uniform radial velocity distribution.

3.2 The FWHM

The systematic uncertainty in the FWHM of Hα is always less than the size of each data point (< 4 km s^{-1}) in the spectra. The random noise in the data is similar to the radial velocity values.

The average FWHM is 50.2 ± 1.8 km s^{-1} for NGC 7000, 49.7 ± 2.8 km s^{-1} for IC 5070 and 50.0 ± 2.1 km s^{-1} for the entire W80 complex. The central parts of NGC 7000 and IC 5070 have a wider FWHM than the other regions. This could be a clue about lower temperature values inside. However, we do not have any information about the emission lines of heavier elements which may further substantiate this conclusion.

3.3 The Intensity

There was approximately a 15% uncertainty in the absolute intensity calibration plus a $\sim$ 9% uncertainty emerging from the sources of random photons in the data obtained from W80. The average intensity is 743 ± 36 R for NGC 7000, 449$\pm$33 R for IC 5070 and 653$\pm$36 R for the W80 complex. A bright line can be seen in Figure 4, which follows a path from north to south of NGC 7000. The night sky brightness is about 250 R. Thus, both NGC 7000 and IC 5070 can be seen in the night sky with the naked eye.

We also calculated EM (in the absence of extinction) from the DEFPOS data integrated over velocities $V_{\rm LSR} < 100$ km s^{-1} using EM$= \int n_{\rm e}^2\, dl = 2.75 T_4^{0.9} I_{\rm H\alpha}$ (pc cm^{-6}), where $n_{\rm e}$ is the local electron density, dl is the distance element to the source region, $I_{\rm H\alpha}$ is the Hα intensity in R and T_4 is the temperature of the gas in units of 10^4 K (Haffner et al. 2003; Reynolds et al. 2005). A temperature of about 8000 K for both regions (NGC 7000 and IC 5070) is consistent with the widths of the Hα, [O I] and [S II] emission lines (e.g., Reynolds 1988). These calculations of EM values are in line with the above calculations and are given in Table 2. The average $\log$(EM) is about 3.1 pc cm^{-6} for the entire W80.

4 COMPARISON WITH OTHER WORKS

4.1 The WHAM

Another Fabry-Perot spectrometer currently in use is the WHAM. Observations with WHAM offer a spectral window within 200 km s^{-1} (about 4 Å near Hα) with a velocity resolution of 8–12 km s^{-1} from a one-degree, spatially integrated beam of the sky (Haffner et al. 2003). With its large-aperture (1° field of view) design and modern CCD technology, WHAM can detect emissions as faint as 0.05 R in a 30 s exposure. The calibrated spectra and velocity interval maps are available and can be downloaded from the WHAM website (*www.wham.astro.wisc.edu*). The WHAM data cover the W80 region with five data points which have galactic coordinates, intensity, $V_{\rm LSR}$ and FWHM values listed in Table 3.

For the WHAM data of the W80 region, mean values for the intensity, $V_{\rm LSR}$ and FWHM are 264.3 R, 2.6 km s^{-1} and 33.2 km s^{-1}, respectively. Comparing the WHAM data and DEFPOS data is not the right approach because of the different FOVs. However, it can be seen that the values for $V_{\rm LSR}$ and FWHM from both instruments are in agreement.

Table 3 The WHAM Data Near the W80 Nebula Complex

l ($^\circ$)	b ($^\circ$)	Intensity (R)	$V_{\rm LSR}$ (km s^{-1})	FWHM (km s^{-1})
84.2820	–0.0027	135.7	4.5	44.8
84.7820	0.8475	73.2	1.0	44.2
85.2621	–0.0027	189.1	3.3	35.3
85.3014	–1.7008	483.3	0.8	40.0
85.7614	–0.8508	311.4	5.1	33.2

4.2 Fountain et al. (1983)

The multiple slit echelle spectrograph observations of Hα were used to map the radial velocities of the W80 complex by Fountain et al. (1983) (hereafter F83). The instrument has a $2' \times 3'$ FOV, a 12.7 cm aperture and a dispersion resolution of 7.25 Å mm^{-1}. They measured the radial velocity and FWHM of the Hα line in different areas of the W80 complex. The mean value of the $V_{\rm HEL}$ for the complex is –15.1±5.5 km s^{-1} and the mean value of FWHM is 28.6±0.6 km s^{-1}. Although we have achieved results that are similar to F83, there was not a close agreement because of differences in the FOV and number of data points. They also reported there was no significant variation in radial velocity.

5 DISCUSSION AND CONCLUSIONS

There are many images from flux calibrated Hα surveys of the northern sky with high spatial resolution, such as the INT Photometric Hα Survey of the Northern Galactic Plane (IPHAS; Drew et al. 2005) and the Virginia Tech Spectral-Line Survey (VTSS; Dennison et al. 1998). Although data from these surveys have better spatial resolution, they do not include velocity information. For this reason, they cannot solely provide sufficient information to understand H II regions. Currently, high spectral and spatial resolution Fabry-Perot spectrometers, such as the scanning Fabry-Perot interferometer (Godbout et al. 1998), Integral Field Spectroscopy (IFS; e.g, Jahnke et al. 2004) and echelle spectrometers (F83), can show small-scale velocity fluctuations (turbulent motion) inside H II regions. However, acquiring these higher resolution data is a challenge because of long exposure times and large sizes of data sets.

The DEFPOS instrument incorporates the advantages of both techniques. It can precisely measure the intensity ($I_{\rm H\alpha}$), line width (FWHM) and radial velocity ($V_{\rm LSR}$) of Hα. Such a spectrometer is a unique tool for investigating the Hα emission line from diffuse sources like H II regions.

By analyzing the DEFPOS data from W80, we find the resulting intensity ($I_{\rm H\alpha}$), line width (FWHM) and radial velocity ($V_{\rm LSR}$) of Hα are in the ranges of 259 to 1159 R, 44 to 55 km s^{-1} and 4 to 12 km s^{-1}, respectively (see Table 2). Their respective average values are 653±36 R, 50.0±2.1 km s^{-1} and 8.2±0.7 km s^{-1}.

The average radial velocity ($V_{\rm HEL}$) is –7.4±0.6 km s^{-1} for NGC 7000, –8.8±0.9 km s^{-1} for IC 5070 and -7.8±0.7 km s^{-1} for the entire W80 complex. F83 found that the mean values of $V_{\rm HEL}$ are –15.4±3.7 km s^{-1} for NGC 7000, –14.8±4.1 km s^{-1} for IC 5070 and –15.1±5.5 km s^{-1} for the entire W80 complex. Also, Hippelein (1973) gave a heliocentric radial velocity of –15.7 and –16.4 km s^{-1} for NGC 7000 and IC 5070, respectively.

The DEFPOS spectrometer has the ability to perform precise measurements, including the radial velocity ($V_{\rm LSR}$) of Hα. However, it cannot obtain detailed information about turbulent motion inside the nebulae because of the relatively wide FOV. Its radial velocity data can be utilized to verify the presence of large-scale velocity gradients. This is apparently in the radial velocity map of the W80 complex (see Fig. 4). Results of earlier works produced a general picture of the dynamics of the W80 complex. No turbulence has been identified in the W80 complex and this is confirmed with the new DEFPOS data.

There are several maxima and minima inside NGC 7000 and IC 5070. The average $\log$(EM) value calculated, using R of Hα, is 3.1 pc cm^{-6} for the entire W80.

The profile plots in Figure 3 for regions 1–6 show bright lines in both $I_{\rm H\alpha}$ and $V_{\rm LSR}$. Moreover, FWHM values from the same regions are also wider. This region shows a circular ionized nebula around an early type star (2MASS J205551.25+435224.6) which represents a classical H II region. This could be verified with the help of more data in other wavelengths.

The 2400 s integration time per beam provided an SNR of 5–20 for the observed 260–1160 R line intensity with widths of 46–55 km s^{-1}. For comparison, note that a 30 s integration time per beam provides an SNR of 20 for a weak 0.5 R line having a width of 20 km s^{-1} (see Tufte 1997).

Using different equipment, our measurements seem to have quite low SNR values. However, these values are good enough to analyze weak diffuse objects that cover a large area.

There is an expected correlation between the $I_{\mathrm{H}\alpha}$ and the FWHM values of the Hα line. However, the same could not be established between either the FWHM and the V_{LSR} or between $I_{\mathrm{H}\alpha}$ and the V_{LSR} values. By repeated observations, changes in physical properties over time could be obtained. This is one of our future aims.

Acknowledgements This work is supported by the Scientific and Technical Research Council of Turkey (TUBITAK) with grant number 104T252 and also by the Scientific Research Project Office of Çukurova University with grant number TBMYO2010BAP4. The author thanks TUBITAK for (partial) support in using RTT150 (project number 08ARTT150-350, 08BRTT150-365 and 11ARTT150-116) and the staff of TUBITAK National Observatory (TUG) for their help. The author would like to thank Ilhami Yegingil and Muhittin Sahan for their valuable guidance, help and advice. The author would also like to thank R. J. Reynolds (University of Wisconsin) for his valuable help in the optical design of the DEFPOS as well as in starting the present study. The author is also grateful to A. Akyuz, M. E. Ozel and A. Abdulvahitoglu for reading and correcting the manuscript and for their valuable remarks.

References

Aksaker, N. 2009, PhD. Thesis, Cukurova University, Adana

Aksaker, N., Sahan, M., Yegingil, I., & Emrahoglu, N. 2011, New Astron., 16, 485

Aksaker, N., Yeğingil, I., & Şahan, M. 2009, Experimental Astronomy, 24, 127

Şahan, M., Yeğingil, I., & Aksaker, N. 2009, RAA (Research in Astronomy and Astrophysics), 9, 237

Coakley, M. M., Roesler, F. L., Reynolds, R. J., & Nossal, S. 1996, Appl. Opt., 35, 6479

Comerón, F., & Pasquali, A. 2005, A&A, 430, 541

Courtès, G., Cruvellier, P., & Pottasch, S. R. 1962, Annales d'Astrophysique, 25, 214

Dennison, B., Simonetti, J. H., & Topasna, G. A. 1998, PASA, 15, 147

Drew, J. E., Greimel, R., Irwin, M. J., et al. 2005, MNRAS, 362, 753

Fich, M., Blitz, L., & Stark, A. A. 1989, ApJ, 342, 272

Fountain, W. F., Gary, G. A., & Odell, C. R. 1983, ApJ, 269, 164

Godbout, S., Joncas, G., & Drissen, L. 1998, PASA, 15, 60

Haffner, L. M., Reynolds, R. J., & Tufte, S. L. 1998, ApJ, 501, L83

Haffner, L. M., Reynolds, R. J., Tufte, S. L., et al. 2003, ApJS, 149, 405

Hausen, N. R., Reynolds, R. J., & Haffner, L. M. 2002, AJ, 124, 3336

Hippelein, H. H. 1973, A&A, 25, 59

Jahnke, K., Wisotzki, L., Sánchez, S. F., et al. 2004, Astronomische Nachrichten, 325, 128

Lynds, B. T. 1962, ApJS, 7, 1

Reynolds, R. J. 1988, ApJ, 333, 341

Reynolds, R. J., Chaudhary, V., Madsen, G. J., & Haffner, L. M. 2005, AJ, 129, 927

Reynolds, R. J., Tufte, S. L., Haffner, L. M., Jaehnig, K., & Percival, J. W. 1998, PASA, 15, 14

Sahan, M., Yegingil, I., Aksaker, N., Kiziloglu, Ü., & Akyilmaz, M. 2005, ChJAA (Chin. J. Astron. Astrophys.), 5, 211

Straižys, V., & Laugalys, V. 2008, Baltic Astronomy, 17, 143

Tufte, S., Reynolds, R., & Haffner, M. 1999, in Interstellar Turbulence, eds. J. Franco, & A. Carraminana (Cambridge: Cambridge Univ. Press), 27

Tufte, S. L. 1997, The WHAM Spectrometer: Design, Performance Characteristics, and First Results, Ph.D. thesis, University of Wisconsin, Madison

Uyanıker, B., Fürst, E., Reich, W., Aschenbach, B., & Wielebinski, R. 2001, A&A, 371, 675

Westerhout, G. 1958, Bull. Astron. Inst. Netherlands, 14, 215

Williamson, R. A. 1970, Ap&SS, 6, 45